J|A|C|S ARTICLES

Published on Web 07/22/2010

A New Family of Nonionic Dendritic Amphiphiles Displaying Unexpected Packing Parameters in Micellar Assemblies

Britta Trappmann,[†,‡,§] Kai Ludwig,[§,||] Michał R. Radowski,[†] Anuj Shukla,[‡] Andreas Mohr,[†] Heinz Rehage,[‡] Christoph Böttcher,*[,||] and Rainer Haag*[,†]

Institut für Chemie und Biochemie, Freie Universität Berlin, Takustrasse 3, 14195 Berlin, Germany, Physikalische Chemie II, Universität Dortmund, Otto-Hahn-Strasse 6, 44227 Dortmund, Germany, and Forschungszentrum für Elektronenmikroskopie, Institut für Chemie und Biochemie, Freie Universität Berlin, Fabeckstrasse 36a, 14195 Berlin, Germany

Received March 1, 2010; E-mail: haag@chemie.fu-berlin.de; christoph.boettcher@fzem.fu-berlin.de

Abstract: In this paper we report on the synthesis of a new family of nonionic dendritic amphiphiles that self-assemble into defined supramolecular aggregates. Our approach is based on a modular architecture consisting of different generations of hydrophilic polyglycerol dendrons [G1−G3] connected to hydrophobic C_{11} or C_{16} alkyl chains via mono- or biaromatic spacers, respectively. All amphiphiles complex hydrophobic compounds as demonstrated by solubilization of Nile Red or pyrene. The structure of the supramolecular assemblies as well as the aggregation numbers are strongly influenced by the type of the dendritic headgroup. While the [G1] amphiphiles form different structures such as ringlike and fiberlike micelles, the [G2] and [G3] derivatives aggregate toward spherical micelles of low polydispersity clearly proven by transmission electron microscopy (TEM) measurements. In the case of the biaromatic [G2] derivative, the structural persistence of the micelles allowed a three-dimensional structure determination from the TEM data and confirmed the aggregation number obtained by static light scattering (SLS) measurements. On the basis of these data, molecular packing geometries indicate a drastic mass deficit of alkyl chains in the hydrophobic core volume of spherical micelles. It is noteworthy that these highly defined micelles contain as little as 15 molecules and possess up to 74% empty space. This behavior is unexpected as it is very different from classical detergent micelles such as sodium dodecyl sulfate (SDS), where the hydrophobic core volume is completely filled by alkyl chains.

Introduction

Nonionic polymeric amphiphiles have attracted special interest due to their tendency to form very stable aggregates and are therefore useful for the efficient solubilization of active agents, for example, in drug delivery.[1] Among them are many biocompatible poly(ethylene glycol)- (PEG-) based surfactants, such as Cremophor, Pluronics, and Tween, which have been extensively used to formulate hydrophobic drugs.[2] Advantages over ionic amphiphiles include their pH independency and the generation of nontoxic nanoparticulate aggregates, which provide a great benefit for drug delivery. However, in contrast to charged amphiphiles, which can assemble into defined aggregates,[3−5] nonionic surfactants have been previously reported to lead to diverse and ill-defined micelles.[1a] Therefore, a remaining challenge is the generation of structurally persistent aggregates[3] that act as stable nanocarriers for hydrophobic drugs and dyes. Because of their low polydispersity and their tunable size, dendritic structures are promising for the construction of new amphiphiles. Grinstaff and co-workers[6] have synthesized dendritic amphiphiles from glycerol, succinic acid, and myristic acid. By varying the hydrophobic-to-hydrophilic ratio and including ionic headgroups, a wide range of aqueous aggregation behavior could be studied but no defined structures were observed. Furthermore, Percec et al. and also Lee and coworkers[7] have shown that aromatic units can drastically enhance the stability of supramolecular assemblies. Depending on the nature of the incorporated hydrophobic branch, hollow as-

† Institut für Chemie und Biochemie, Freie Universität Berlin.
‡ Universität Dortmund.
§ B.T. and K.L. contributed equally.
|| Forschungszentrum für Elektronenmikroskopie, Institut für Chemie und Biochemie, Freie Universität Berlin.

(1) (a) Schick, M. J. *Nonionic Surfactants: Physical Chemistry*; CRC Press: Boca Raton, FL, 1987. (b) Haag, R. *Angew. Chem., Int. Ed.* **2004**, *43*, 278–282.
(2) Kabanov, A. V.; Alakhov, V. Y. *Crit. Rev. Ther. Drug Carrier Syst.* **2002**, *19*, 1–72.
(3) Kellermann, M.; Bauer, W.; Hirsch, A.; Schade, B.; Ludwig, K.; Böttcher, C. *Angew. Chem., Int. Ed.* **2004**, *43*, 2959–2962.
(4) Burghardt, S.; Hirsch, A.; Schade, B.; Ludwig, K.; Böttcher, C. *Angew. Chem., Int. Ed.* **2005**, *44*, 2976–2979.
(5) Schade, B.; Ludwig, K.; Böttcher, C.; Hartnagel, U.; Hirsch, A. *Angew. Chem., Int. Ed.* **2007**, *46*, 4393–4396.
(6) (a) Luman, N. R.; Grinstaff, M. W. *Org. Lett.* **2005**, *7*, 4863–4866. (b) Meyers, S. R.; Juhn, F. S.; Griset, A. P.; Luman, N. R.; Grinstaff, M. W. *J. Am. Chem. Soc.* **2008**, *130*, 14444–14445.
(7) (a) Percec, V.; Peterca, M.; Dulcey, A. E.; Imam, M. R.; Hudson, S. D.; Nummelin, S.; Adelman, P.; Heiney, P. A. *J. Am. Chem. Soc.* **2008**, *130*, 13079–13094. (b) Kim, J.-K.; Lee, E.; Huang, Z.; Lee, M. *J. Am. Chem. Soc.* **2006**, *128*, 14022–14023. (c) Percec, V.; Dulcey, A. E.; Balagurusamy, V. S. K.; Miura, Y.; Smidrkal, J.; Peterca, M.; Nummelin, S.; Edlund, U.; Hudson, S. D.; Heiney, P. A.; Duan, H.; Magonov, S. N.; Vinogrador, S. A. *Nature* **2004**, *430*, 764–768. (d) van Dongen, S. F. M.; De Hoog, H.-P. M.; Peters, R. J. R. W.; Nallani, M.; Nolte, R. J. M.; van Hest, J. C. M. *Chem. Rev.* **2009**, *109*, 6212–6274. (e) Rosen, B. M.; Wilson, C. J.; Wilson, D. A.; Peterca, M.; Imam, M. R.; Percec, V. *Chem. Rev.* **2009**, *109*, 6275–6540.

Scheme 1. Synthesis, Structure, and Aggregation of Aromatic Dendritic Amphiphiles[a]

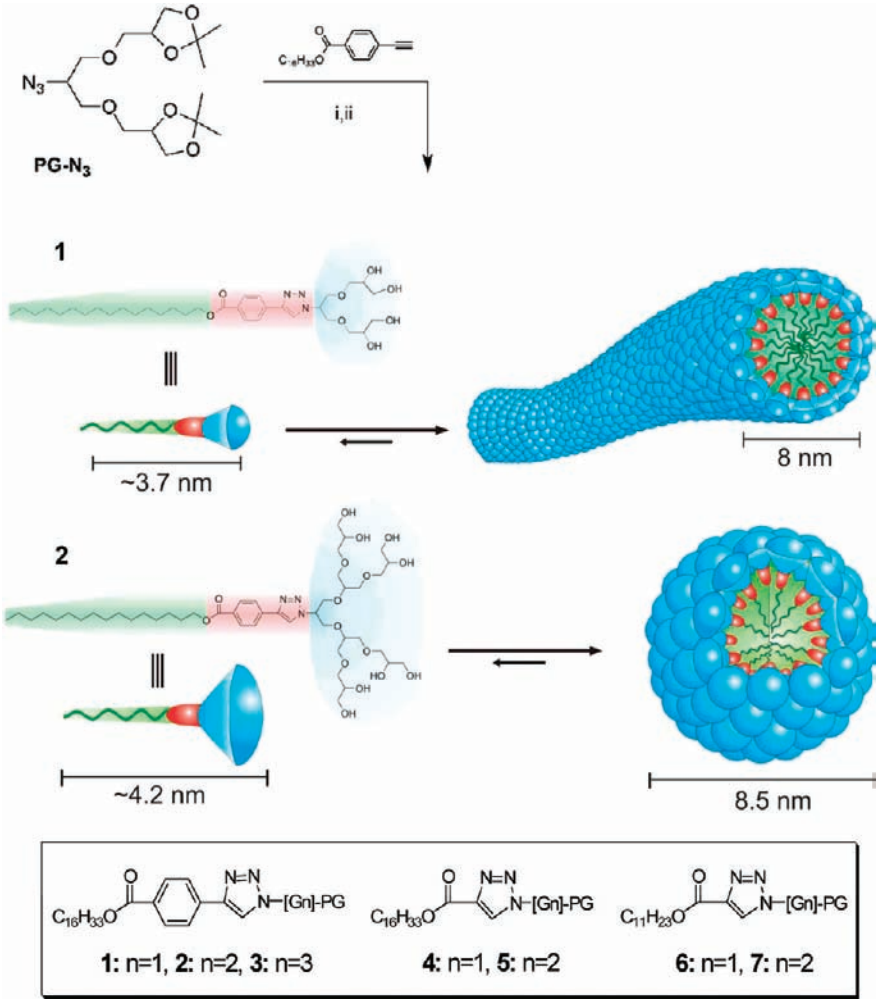

[a] PG represents different generations of polyglycerol dendrons. (i) 5 mol % $CuSO_4$, 10 mol % ascorbic acid, 30 mol % NaOH, THF/H_20 1:1, rt, 2−5 days; (ii) Lewatit K1131, MeOH, 24 h, rt. Umbrella-shaped molecular geometry of spacious G2 headgroups induces high-curvature spherical micelles, whereas less voluminous G1 dendrons promote linear growth toward fibrous assemblies. This behavior is independent of the aromatic spacer and the alkyl chain length used in this study (cf. Table 1).

semblies or long cylindrical micelles can be formed. Recently, we have also observed the strong influence of aromatic units on the solubilization of hydrophobic guest molecules within dendritic core−shell architectures.[8] Therefore, our structural design for this study was to combine nonionic dendritic and aromatic units with long alkyl tails in order to control the formation of structurally defined and stable micelles with good transport properties for hydrophobic guest molecules.

Herein we report on a modular approach for the synthesis of a new family of nonionic dendritic amphiphiles. This approach is based on a modular architecture consisting of different generations of polyglycerol dendrons [G1−G3] as hydrophilic parts connected to C_{16} or C_{11} alkyl chain as hydrophobic units via mono- or biaromatic spacers, respectively (Scheme 1).

The dendrimers showed self-assembly into different supramolecular architectures depending on their molecular structure with unexpected packing parameters. The aim of this study is to gain insight into the molecular factors governing self-assembly and to survey the transport behavior for hydrophobic guest molecules in water. Surprisingly, we found that the dendritic headgroups are capable of imposing the formation of structural persistent assemblies, which is the first example to be proven for nonionic amphiphiles.

Results and Discussion

We designed a modular approach that allows for a facile synthesis of structurally varied compounds represented by the amphiphiles **1**−**7**, making use of "click" coupling as a highly reliable step for scale-up of the process. This study is focused on preselected dendritic amphiphiles that differ in the size of the hydrophilic headgroup by using different generations of polyglycerol dendrons.[9]

As starting materials, we chose acetal-protected [G1] to [G3] polyglycerol dendron azides as hydrophilic building blocks and propionic acid alkyl ester or 4-ethynylbenzoic acid alkyl ester as hydophobic units. The synthesis of all dendritic polyglycerol monoazides was carried out via a previously reported procedure.[9] The acetal protecting groups were removed in the last step to obtain the active amphiphiles **1**−**7** (Scheme 1).

At first we studied the aggregation behavior of our new dendritic nonionic amphiphiles in detail using different physical

(8) Türk, H.; Shukla, A.; Rodrigues, P. C. A.; Rehage, H.; Haag, R. *Chem.—Eur. J.* **2007**, *13*, 4187–4196.

(9) Wyszogrodzka, M.; Haag, R. *Chem.—Eur. J.* **2008**, *14*, 9202–9214.

Table 1. Critical Micelle Concentrations, Aggregation Numbers and Hydrodynamic Diameters,[a] and Diameters[b] of Dendritic Amphiphiles **1**−**7**

compd	cmc (M)	ST + SLS aggregation number[c]	DLS hydrodynamic diameter[d] (nm)	TEM diameter (nm)
1 [G1]	1.5×10^{-5}	na[e]	na[e]	8.0 ± 1.0 (fibers)
2 [G2]	1.1×10^{-5}	60 ± 2	8.1 ± 0.4	8.5 ± 1.0
3 [G3]	7.1×10^{-6}	21 ± 2	7.2 ± 0.4	6.5 ± 1.0
4 [G1]	3.7×10^{-5}	na[e]	na[e]	7.7 ± 1.0 (fibers)
5 [G2]	9.0×10^{-6}	42 ± 2	7.3 ± 0.4	6.8 ± 2.0
6 [G1]	1.4×10^{-4}	na[e]	na[e]	5.7 ± 1.0 (fibers)
7 [G2]	6.4×10^{-4}	15 ± 2	5.3 ± 0.3	5.2 ± 2.0

[a] From light scattering data. [b] From TEM data. [c] Error values were based on linear regression analysis and determined in the context of the Excel RGP function. [d] Hydrodynamic diameters of spherical micelles (values of intensity mean peak distribution). Values of error result from three consecutive measurements of the same sample, and the corresponding standard deviations are given. Deviations between two measurements performed over a time lag of 6 months were within the given error margin. [e] Due to the formation of fiber aggregates of different length, measurement of the hydrodynamic diameter and determination of the aggregation numbers for [G1] derivatives became nonapplicable.

characterization methods such as surface tension measurements, static and dynamic light scattering (SLS and DLS), cryogenic transmission electron microscopy (cryo-TEM), and image processing techniques. Subsequently the transport capacities of the amphiphilic aggregates were tested.

Surface tension measurements were performed in a pendant drop apparatus. Surface tension data were plotted as a logarithmic function of the surfactant concentration, where a break in the curve occurs at the critical micelle concentration (cmc). Thus, the influence of the PG generations, the size of the aromatic spacer, and the length of the alkyl chains were compared (Scheme 1, Table 1).

The cmc for the biaromatic compounds **1**, **2**, and **3** differing in the size of the dendritic headgroup are 1.5×10^{-5}, 1.1×10^{-5}, and 7.1×10^{-6} M, respectively. This trend shows that a larger degree of hydrophilicity leads to lower cmc values. A similar observation has already been made by Eisenberg and co-workers[10] for amphiphilic block copolymers composed of styrene and sodium acrylate, where the cmc decreases with increasing size of the hydrophilic unit. The shortening of the alkyl chain length from C_{16} to C_{11} chains also shows a significant impact on the cmc if we compare, for example, the corresponding values of **5** (9.0×10^{-6} M) and **7** (6.4×10^{-4} M), respectively. Here the larger degree of hydrophobicity leads to a significantly lower cmc. However, the shortening of the aryl spacer (although considered to be an integral part of the hydrophobic segment) has obviously no significant effect on the cmc if we compare the [G2] derivatives **2** and **5** with bi- and monoaromatic spacers, respectively. Here the impact of the alkyl chain might be dominating.

The aggregation of the amphiphiles was confirmed by light scattering data, which allowed determination of the hydrodynamic diameters as well as the aggregation numbers (Table 1). In order to complement the aggregation phenomena by direct structural data, cryo-TEM was performed for aqueous sample solutions at a general concentration of 1.0×10^{-3} M, which is well above the compounds' corresponding cmc values. It can clearly be seen that hydrodynamic diameters determined from dynamic light scattering data and mean diameters obtained from TEM measurements are highly consistent in the case of the [G2] and [G3] derivatives **2**, **3, 5**, and **7** as we observed uniform spherical micellar aggregates for them (for a detailed analysis see below).

[G1] derivatives **1**, **4**, and **6** behave differently, which is already apparent by their poor solubility in water. For example, compound **1** can only be dissolved in water at higher temperatures (above 70 °C) where an almost clear solution (a faint opacity is retained) is obtained. Upon cooling to room temperature, the solution becomes viscous but remains clear for at least ~12 h before visible precipitation occurs. By repeated cryo-TEM measurements we observed that multiple heating−cooling cycles of the sample affect the appearance of the aggregate structure, particularly with regard to the aggregate shape and size (Figure 1A). From the first cycle, predominantly fibrous micelles with a uniform diameter of ~8 nm were obtained. The length of the fibers varied from 15 nm up to several hundred nanometers. In later cycles, smaller micellar aggregates of ~14 nm diameter became dominant (Figure 1B). Tilt experiments showing the assemblies at different angles (see Supporting Information) confirmed the impression that the micellar organization is of ringlike geometry. Figure 1B shows both fibers as well as ringlike micelles within one single micrograph. However, the heterogeneity of the aggregates explains the average aggregate size of 11.5 nm obtained from DLS data. We therefore conclude that the scattering data and the determination of the aggregation numbers are not reliable in this case. The [G1] derivatives **4** and **6** show a similar behavior even though the solubility is slightly better due to the shorter hydrophobic building block. Fibers and spherical micelles can also be found here (Figure 1A,C).

Most interestingly, spherical micelles formed by amphiphile **2** showed a well-resolved internal structure upon closer inspection of the electron microscopic data (Figure 1, bottom row). It was supposed that the differences in the ultrastructural pattern represent different spatial views of the assemblies and might be used to determine their three-dimensional organization, as has been demonstrated earlier for structurally persistent micelles of different *ionic* calixarene and fullerene dendrimers.[3−5] By use of the cryo-negative staining sample preparation procedure,[11] the contrast of these structural details can be enhanced (Figure 1C). Image processing techniques were applied and alignment and classification algorithms were used to reconstruct the three-dimensional volume of the micelle. The obtained three-dimensional structure determined for [G2] micelles is shown in a surface representation in Figure 2. The micelle is characterized by D_3 symmetry and shows a specific arrangement of 20 equal high-density patches distributed over the outer micellar corona. The interior core volume thought to accommodate the hydrophobic alkyl chains appears hollow. This is an expected phenomenon as the reconstruction is based on averaging methods that consider only structurally identical aggregate features. The alkyl chains, however, are known to be highly flexible (fluidlike) and therefore do not contribute structural information to the reconstruction.

If the reconstructed micelle is viewed along the 3- and 2-fold axes, respectively, the slightly oblate geometry becomes clearly visible. Here, the shorter dimension (7.8 nm) of the micelle corresponds perfectly to a bilayer arrangement of the am-

(10) Astafieva, I.; Zhong, X. F.; Eisenberg, A. *Macromolecules* **1993**, *26*, 7339–7352.

(11) De Carlo, S.; El-Bez, C.; Alvarez-Rua, C.; Borge, J. *J. Struct. Biol.* **2002**, *138*, 216–226.

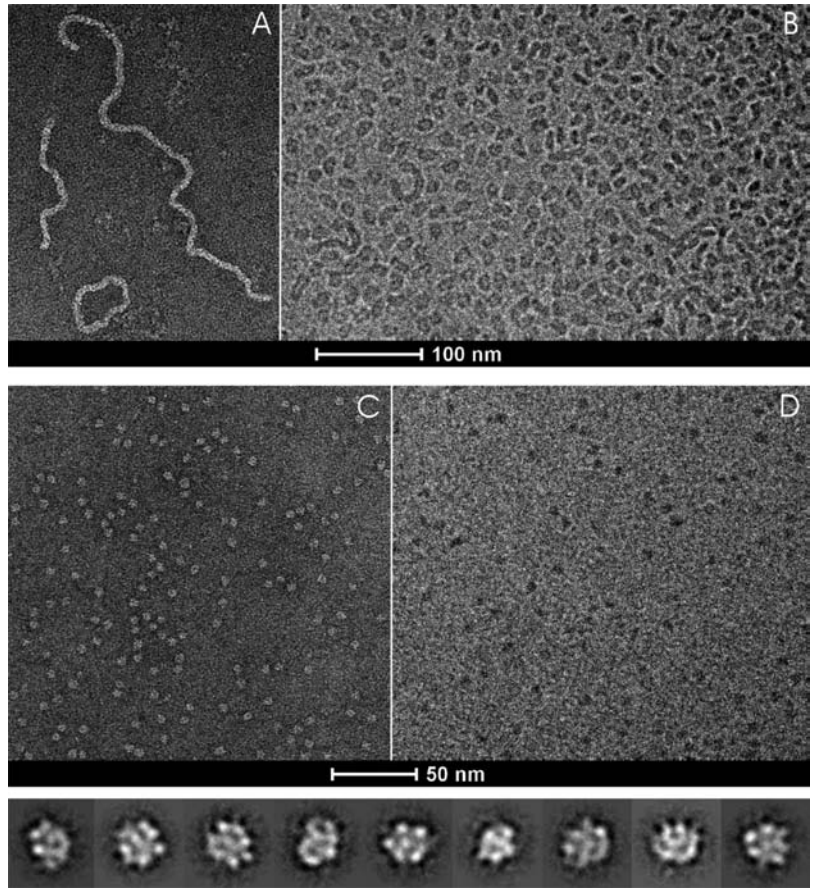

Figure 1. (A) Cryo-negative stain and (B) cryo-TEM image of an aqueous solution of the dendritic amphiphile **1** ([G1] derivative). Fiberlike and ringlike micelles in different orientations are clearly visible. Tilting experiments confirm the ringlike character of the micelles (see Supporting Information). Fiber assemblies have a diameter of about 8 nm, which roughly corresponds to a molecular bilayer, whereas diameters of the ring micelles are on the order of up to 14 nm, depending on the micelles' spatial orientation. (C) Cryo-negative stain and (D) cryo-TEM micrograph showing the vitrified sample of amphiphile **2** at a concentration of 2.5 mg mL^{-1}. Spherical micelles of 8−9 nm in diameter are clearly visible. Differences in shape and size are due to different spatial orientation of the micelles in the frozen sample volume. (Bottom row) Ultrastructural details of the micelles can be extracted by using the cryo-negative staining data in combination with image processing procedures. The gallery shows a selection of class sum images representing different spatial orientations of the micelles.

phiphiles. The maximum extension of the micelle, however, amounts to 8.8 nm. The resolution value of 1.4 nm that we achieved by evaluating a data set of ~8000 individual particles of the [G2] derivative raises the question of what does the data tell us on the molecular level. With the aggregation number of 60 molecules per micelle from the scattering data, we should accommodate three molecules in each of the 20 high-density patches constituting the reconstructed micelle. Figure 2B shows an arrangement of three [G2] amphiphiles in close association with a corresponding surface representation limited at a resolution value of 1.4 nm (to meet the information content of the reconstruction) by applying adequate filter parameters (Gaussian filtered by use of SITUS software). It is obvious that the three dendritic headgroups generate a triangular cone, although the typical features of the dendritic peculiarity are blurred. It is noticeable (and in accordance with the reconstruction) that the hydrophobic alkyl chains are barely visible at this resolution level. However, the triangular cones fit perfectly into the three-dimensional reconstruction (see Figure 2C), so that we end up with $20 \times 3 = 60$ molecules forming the reconstructed micelle.

In all cases where the hydrodynamic diameters were determined for spherical micelles by dynamic light scattering measurements, we observed very good agreement with the mean diameters obtained from the TEM data. A general trend is indicated in the examined series of compounds. By increasing the spatial demand of the headgroup, the aggregation number and hence the micellar diameter decreases. This trend endures if the aromatic spacer (**4** and **5**) or the alkyl chains (**6** and **7**) are shortened. Spherical micelles of **5** [again the [G1] derivative **4** forms fiberlike aggregates (Figure 1a in Supporting Information) like **1**] have a smaller diameter, which can be expected because of the shortening of the spacer. Here, the higher curvature permits a smaller aggregation number of about 42 amphiphiles. If we assume analogous packing conditions as were observed in the case of the biaromatic compound **2**, we would expect accurately this value. The aggregates of the biaromatic [G2] amphiphile **2**, however, turned out to be a unique case where the structural persistence allowed for a consistent three-dimensional reconstruction. Structural identity of all assemblies (8700 randomly selected assemblies were used in the reported case here) is a precondition for a successful application of the approach, which method includes a multivariate statistical analysis of the data set (see also Supporting Information for details). We suspect that the dimensions of alkyl chains, spacer, and headgroup geometry constitute a unique balance in the case of **2**, which made the formation of structurally persistent[3] aggregates possible. In all other cases (compounds **3**, **5**, and **7**), this criterion is not fulfilled, which became apparent from the multivariate statistical analysis and classification involved in the image processing procedure showing that the assemblies

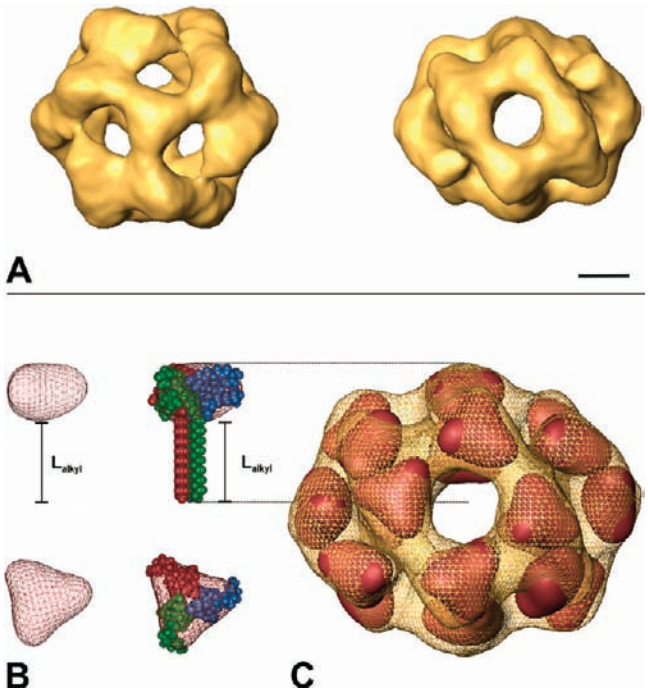

Figure 2. (A) Three-dimensional reconstruction (surface representation) in top (left) and side (right) views obtained from the structural data of ~8000 micelles formed by **2**. Bar is 2 nm. The reconstruction is orientated with respect to the 3-and 2-fold symmetry axes of the inherent D_3 point group symmetry. (B) Trimeric arrangement of [G2] amphiphiles together with a low-resolution depiction in side- and top-view orientation thought to represent the building blocks of the micellar arrangement. (C) Arrangement of the trimeric building blocks shown in panel B within the reconstructed micellar volume. Altogether 60 molecules can be accommodated within the micelle, which is in agreement with the aggregation number obtained from scattering data.

are not strictly monodisperse. Differences in the aggregate size and structural organization of the molecules prevent the calculation of a consistent three-dimensional volume, as structural identity is a precondition for the application of the approach (see above). We therefore conclude that the aggregates are polydisperse to some extent.

These findings, however, have to be discussed in the context of the scattering data. The intensity and volume size distribution data and plots from micellar aggregates are shown in the Supporting Information. In the case of compounds **3**, **5**, and **7**, a relatively broad size distribution is due to the polydispersity of the assemblies proven by TEM.

From the 3D reconstruction of **2**, however, we know that the micelles are not ideal spherical particles but are flattened in one direction (compare top and side views in Figure 2). Such differences in the aggregate geometry obviously result in a slight broadening of the corresponding size distribution, though the micelles are highly monodisperse as proven by the image data processing. One should note that all intensity plots indicate a second peak at a particle size >100 nm. For small, isotropic particles the scattering intensity from a spherical particle is proportional to the size to the sixth power. Therefore, there is a strong overemphasis of bigger particles in the intensity distribution.

However, from the volume distributions (Figure 1b in Supporting Information), it can be inferred that their absolute numbers must be small. As the polydispersity index (PDI) values (in the range of 0.28−0.69) appear to represent the average of a mixture of several species, complementary microscopic analysis is needed to provide a clear picture. Larger aggregates in the 30−150 nm range, however, are also detectable by TEM and appear as unstructured agglomerates (see Figure 8 in Supporting Information). Their number is also here very limited and in the parts per million (ppm) range. Due to the minor importance of the large particles in the context of our observations, we abandon them from a detailed discussion.

The general trend in terms of micellar dimensions, however, is also clearly in line with expectations if the alkyl chain length is shortened from C_{16} to C_{11}. Apart from the fiber formation of the [G1] derivative **6** (note that the diameter of the fibers decreases in accordance with the shortening of the molecular length), spherical micelles (proven by TEM) of the [G2] derivative **7** possess a significantly smaller diameter of about 5.4 nm if compared to the long-chain derivative **5**. Consequently, a lower aggregation number of only 15 amphiphiles is found by SLS due to the high curvature of the small aggregates.

Irrespective of the exact supramolecular organization of the amphiphiles in a micelle, it is obvious from the molecular dimensions alone that there is a clear difference in the spatial demand between the voluminous dendrons and the linear hydrophobic chains, which creates a more or less umbrellalike molecular geometry, particularly in the case of the [G3] amphiphile (see Scheme 1). The aggregation of such molecules has been theoretically rationalized by the concept of the *molecular packing parameter* introduced by Israelachvili et al.[12] This concept is based on geometrical considerations and makes it possible to predict the shape and size of equilibrium associates. Therefore, an increase in the headgroup area of amphiphiles (wedge angle of the dendron) leads to a decrease in the aggregation number, whereby particle size remains almost constant. The general trend predicted by the molecular packing parameter is also valid for our new dendritic amphiphiles, although a number of structural aspects are surprising. The shielding of the corresponding aromatic spacer by the headgroups in the aggregates and thus their spatial separation is definitely supported by corresponding absorption spectra. We found, for example, no indication for $\pi-\pi$ interactions of the biaromatic spacer in the case of **2**, below and above the cmc, neither in freshly prepared nor in months old solutions. However, it appeared very obvious from the umbrella-shaped geometry of the molecules that the contribution to the hydrophobic volume (e.g., of 60 molecules in the micelles of **2**) would be very limited, particularly if the molecules are arranged in a spherical assembly. By simulating the fitting of 60 *complete* molecules (headgroups and alkyl chains) into the reconstructed volume, we notice that the hydrophobic parts do not entirely fill out the interior volume of the micelle. Volume calculations give a noticeable low volumetric efficiency of only 24%. This is in utter difference to "classic" detergent micelles (i.e., SDS). We have measured an SDS solution and determined an aggregation number of 58 ± 8, which is in good agreement with the literature. Sixty SDS molecules at a micelle diameter of 3.8 nm were reported by Turro and Yekta.[13] However, volume calculations reveal that the hydrophobic chains completely occupy the interior core volume of the SDS micelle.

We conclude that the interaction of space-demanding dendritic polyglycerol headgroups dominates the assembly process very clearly. Therefore, the special umbrella-shaped geometry of the

(12) (a) Israelachvili, J. N.; Mitchell, D. J.; Ninham, B. W. *J. Chem. Soc., Faraday Trans. 2* **1976**, *72*, 1525–1568. (b) Kratzat, K.; Finkelmann, H. *Langmuir* **1996**, *12*, 1765–1770.
(13) Turro, N. J.; Yekta, A. *J. Am. Chem. Soc.* **1978**, *100*, 5951.

Table 2. Transport Capacities and Efficiencies of Dendritic Micelles for Solubilizing the Hydrophobic Compounds Nile Red and Pyrene

Compound [hydrophilic head group]	Transport Capacity [mmol/mol]		Transport Efficiency [mg/g]		Structural formula
	Nile Red	Pyrene	Nile Red	Pyrene	
1 [G1]	26.5	72.5	13.3	23.1	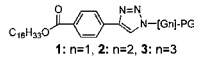
2 [G2]	36.0	82.3	12.3	17.9	**1**: n=1, **2**: n=2, **3**: n=3
3 [G3]	32.3	80.8	6.8	10.7	
4 [G1]	20.9	57.7	11.9	20.8	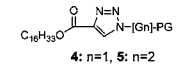
5 [G2]	15.7	75.1	5.8	17.7	**4**: n=1, **5**: n=2
6 [G1]	9.5	28.7	6.2	11.9	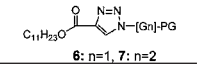
7 [G2]	7.1	2.0	2.8	7.8	**6**: n=1, **7**: n=2

dendritic molecules does not principally allow for a complete filling of the interior micelle core. This conclusion is supported by both characterization methods used (TEM and DLS), as the micelle diameter (as well as the aggregation number for **2**) was confirmed independently by both techniques. Interestingly, the above observations are confirmed for all dendrimer generations in which spherical micelles are formed. For example, if 21 molecules of [G3] amphiphile **3** are accommodated in a spherical micelle of 7 nm diameter, a similar low volumetric efficiency of 26% is obtained. Compounds **5** and **7** show similar behavior with 45% and 32% efficiency, respectively.

One can at present only speculate about the nature of the micellar core. From plausible reasons we exclude vacuum as an explanation. An additional filling with water molecules might be an alternative suggestion, which has been discussed for classical detergent micelles since the mid-1980s.[14] Evidence for the presence of structured water within the hydrophobic core of membranes was, for example, reported by Meier et al.[15] At least an alternative molecular organization such as a vesicle can be ruled out. Although vesicle formation might explain an explicit water-filled interior volume, there are no structural indications such as a bilayered membrane. Moreover, when the voluminous headgroup geometry is taken into account, vesicle formation is barely possible within the boundary of 5−9 nm spheres.

In addition to structural studies, the transport properties of all amphiphiles were investigated by uptake of hydrophobic dyes such as Nile Red and pyrene in water. To establish a structure−transport relationship, the quantities of solubilized Nile Red and pyrene were compared (Table 2). It turns out that the amphiphiles **1**, **2**, and **3** with a biaromatic spacer show relatively high transport capacities (here defined as millimoles of guest molecule per mole of amphiphile). This is in line with our previous report on dendritic core−shell architectures based on hyperbranched polyglycerol-containing biphenyl units for the efficient transport of hydrophobic compounds.[8] In fact, a comparison of amphiphiles **2** and **5** demonstrates increased transport capacities with increased number of aromatic units, with a more than 2-fold increase in solubilized dye when comparing one and two aromatic units. On the other hand, the size of the hydrophilic polyglycerol headgroup has little effect on the transport capacity, but the transport efficiency (here defined as milligrams of guest molecule per gram of amphiphile) decreases with the increasing molecular weight of the growing dendron headgroups [G1]−[G3]. Amphiphiles **6** and **7** with shorter (C_{11}) hydrophobic chains transport much less than all other amphiphiles with longer (C_{16}) chains. It is noteworthy that the pure aromatic guest pyrene is solubilized much better (up to 5 dye molecules per [G2] micelle) than the heterocyclic dye Nile Red (only up to 2 dye molecules).

As we observed a prominent alteration of the micellar structure upon uptake of hydrophobic guest molecules in the case of ionic dendrimers,[16] we also analyzed the loaded nonionic systems by TEM. However, the data revealed no significant size change upon guest loading, neither with Nile Red nor with pyrene. This finding might be another indication that the sparsely populated hydrophobic micellar core offers sufficient space for an uptake of guest molecules without alteration of the overall structure.

Conclusions

We have developed a new family of dendritic amphiphiles that undergo controlled aggregation at very low critical micelle concentrations. All amphiphiles were tested as potential nanocarriers for hydrophobic compounds and were shown to entrap the dyes Nile Red and pyrene. Different structural parameters influencing the transport and aggregation behavior were investigated. It was shown that the aromatic spacers of the amphiphile play an important role for the transport of aromatic guest molecules. Furthermore, the aggregation number is strongly influenced by the dendritic headgroup, which leads to structurally persistent and highly defined spherical micelles for [G2] dendrons. Also, the structurally more defined [G2] micelle (60 amphiphiles) shows much better transport efficiencies due to the higher order compared to other structurally less defined assemblies.

This is the first example for structurally highly defined micelles based on nonionic surfactants consisting of as little as 15 dendritic amphiphiles. The most exciting and novel aspect of our study is the unquestionable alkyl chain volume deficit in the micelles' hydrophobic core, which has been proven by two independent methods. This finding spurs on further studies characterizing and explaining this supramolecular phenomenon as well as the synthesis of new dendritic supramolecular assemblies with unique properties.

Acknowledgment. This work was supported by the SFB 765 from the Deutsche Forschungsgemeinschaft. Also, the Studienstiftung des Deutschen Volkes is kindly acknowledged for a scholarship to B.T. We also thank A. Wiedekind for repititive DLS measurements and W. Münch for HPLC purification of dendritic amphiphiles.

Supporting Information Available: Experimental Section and additional text, 9 figures, and one table describing purification and characterization details of dendritic amphiphiles **1**−**7**, light scattering data, determination of the transport capacity for Nile Red, and additional TEM data. This material is available free of charge via the Internet at http://pubs.acs.org.

JA101523V

(14) (a) Dill, K. A.; Koppel, D. E.; Cantor, R. S.; Dill, J. D.; Bendedouch, D.; Chen, S. H. *Nature* **1984**, *309*, 42–45. (b) Menger, F. M.; Doll, D. W. *J. Am. Chem. Soc.* **1984**, *106*, 1109–1113.

(15) Meier, E. M.; Schummer, D.; Sandhoff, K. *Chem. Phys. Lipids* **1990**, *55* (2), 103–113.

(16) Jäger, C. M.; Hirsch, A.; Schade, B.; Ludwig, K.; Böttcher, C.; Clark, T. *Langmuir* **2010**, *26* (13), 10460–10466.